TWO CHARACTERISIC VOLUMES IN MULTIFRAGMENTATION OF HOT NUCLEI

V.A.Karnaukhov[1], H.Oeschler[2], A.Budzanowski[3], S.P.Avdeyev[1], V.V.Kirakosyan[1], V.K.Rodionov[1], P.A. Rukoyatkin, A.V.Simonenko[1], W.Karcz[3], I.Skwirczynska[3], E.A.Kuzmin[4], E.Norbeck[5], A.S.Botvina[6]

[1]Joint Institute for Nuclear Research, Dubna, Russia; [2] Institut für Kernphysik, University of Technology, Darmstadt, Germany; [3] H.Niewodniczanski Institute of Nuclear Physics, Cracow, Poland; [4] Kurchatov Institute, Moscow,Russia; [5] University of Iowa, Iowa City, USA; [6] Institute for Nuclear Research, Moscow, Russia

Thermal multifragmentation of hot nuclei is interpreted as the nuclear *liquid-fog* phase transition inside the spinodal region. The exclusive data for *p*(8.1GeV) + Au collisions are analyzed within the framework of statistical model (SMM). It is found that the partition of hot nuclei is specified after expansion to a volume equal to $V_t = (2.6 \pm 0.3)\ V_o$. The kinetic freeze-out volume is found to be twice as large: $V_f = (5 \pm 1)\ V_o$. The similarity between multifragmentation and ordinary fission is discussed.

1. THERMAL MULTIFRAGMENTATION AND NUCLEAR FOG

The study of the decay of very excited nuclei is one of the most challenging topics of nuclear physics giving access to the nuclear equation of state for the temperatures below T_c – the critical temperature for the liquid-gas phase transition. The main decay mode of very excited nuclei is a copious emission of intermediate mass fragments (IMF), which are heavier than α-particles but lighter than fission fragments. The great activity in this field has been stimulated by the expectation that this process is related to a phase transition in nuclear media. An effective way to produce hot nuclei is reactions induced by heavy ions with energies up to hundreds of MeV per nucleon. But in this case the heating of the nuclei is accompanied by compression, strong rotation, and shape distortion, which may essentially influence the decay

properties of hot nuclei. One gains the simplicity, and picture becomes clearer, when light relativistic projectiles (protons, antiprotons, pions) are used. In this case, fragments are emitted by only one source – the slowly moving target spectator. Its excitation energy is almost entirely thermal. Light relativistic projectiles provide therefore a unique possibility for investigating *thermal multifragmentation*. The decay properties of hot nuclei are well described by statistical models of multifragmentation [1, 2] and this can be considered as an indication that the system is thermally equilibrated or, at least, close to that. For the case of peripheral heavy ion collisions the partition of the excited system is also governed by heating.

In a number of papers, multifragmentation of hot nuclei is considered as spinodal decomposition. The appearance of the unstable spinodal region in the phase diagram of the nucleonic system is a consequence of the great similarity between nucleon-nucleon and van der Waals interactions [3-5]. The equations of state are similar for these systems, which are tremendously different in respect to the size and energy scales. One can imagine that a hot nucleus (at T = 7-10 MeV) expands due to thermal pressure and enters the unstable region. Due to density fluctuations, a homogeneous system is converted into a mixed phase consisting of droplets (IMF) and nuclear gas interspersed between the fragments. Thus the final state of this transition is a *nuclear fog* [5], which explodes due to Coulomb repulsion and is detected as multifragmentation. It is more appropriate to associate the spinodal decomposition with the *liquid-fog* phase transition in a nuclear system rather than with the *liquid-gas* transition, as stated in several papers (e.g. [6-9]). This scenario is evidenced by the observations:

(a) density of the system at the break-up is much lower than the normal one r_o;

(b) the life-time of the fragmenting system is very small ($\approx$ 50 fm/c), it is of the order of the mean time of density fluctuations [10];

(c) break-up temperature is lower than the critical temperature for the *liquid-gas* phase transition, which is found to be T_c = (17 ± 2) MeV [10].

The first point from this list requires more detailed study. There are a number of papers with estimates of the characteristic volume, but the values obtained deviate significantly [7, 12-15]. In our papers [16,17], the inclusive and exclusive data on the charge distribution and kinetic energy spectra of IMFs produced in *p*(8.1 GeV) + Au collisions were analyzed using the statistical multifragmentation model SMM. It is concluded that one should use *two* volume characteristics, not just *one*, as in traditional approach. The first, $V_t \sim 2.6V_o$ (or $\rho_t \sim 0.38\rho_o$), corresponds to the stage of fragment formation inside the spinodal region (Fig.1).

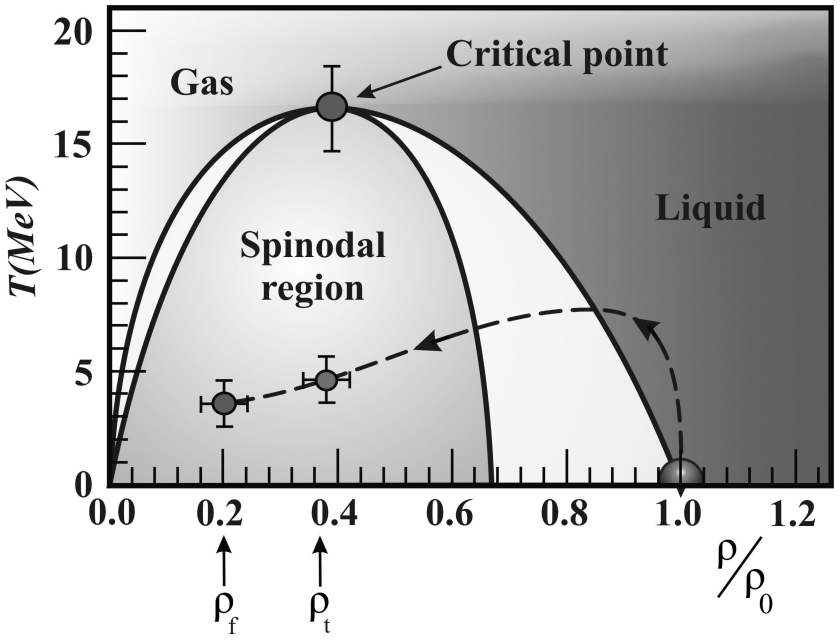

Fig.1. Proposed spinodal region for nuclear system. The experimental points were obtained by the FASA collaboration. The arrow line shows the way of the system from the starting point at T=0 and ρ_o to the break-up configuration at ρ_t and freeze-out point at the mean density ρ_f.

The second one, $V_f \sim 5\ V_o$, is the freeze-out volume. At this configuration, fragments are well separated each other, they are interacting via the Coulomb force only. The first parameter is

obtained by analyzing the IMF charge distributions, the second one is found via measuring the fragment kinetic energy spectra. Experimental data have been obtained using the 4p-device FASA installed at the external beam of the Nuclotron (Dubna). The present setup consists of 30 *dE-E* telescopes surrounded by a fragment multiplicity detector (FMD), which is composed by 58 scintillation counters with thin CsI(Tl).

2. VOLUME FROM IMF CHARGE DISTRIBUTIONS

The reaction mechanism for light relativistic projectiles is usually divided into two stages. The first is a fast energy-depositing stage during which very energetic light particles are emitted and the target spectator is excited. We use the intranuclear cascade model (INC) [18] for describing the first stage. The second stage is considered within the framework of the SMM, which describes multi-body decay (volume emission) of a hot and expanded nucleus. But such a two-stage approximation fails to predict the measured fragment multiplicity. To overcome this difficulty, an expansion stage is inserted. The residual (after INC) masses and their excitation energies are tuned (on event-by-event basis) to obtain agreement with the measured mean IMF multiplicity [19]. This is the INC+Exp+SMM combined model.

The break-up (or partition) volume is parameterized in the SMM as $V = (1+k)\,V_o$. It is assumed in the model that the freeze-out volume, defining the total Coulomb energy of the final channel, coincides in size with the system volume when the partition is specified. Within this model the probabilities of different decay channels are proportional to their statistical weights (exponentials of entropy). The entropy is calculated using the liquid-drop model for hot fragments. The statistical model considers the secondary disintegration of the excited fragments to get the final charge distribution of cold IMFs. The importance of the secondary decay stage is analyzed in Ref. [10].

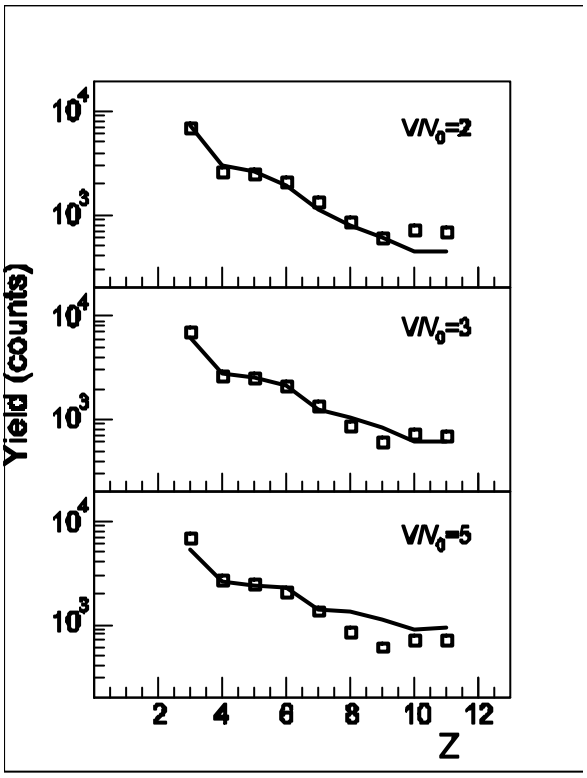

Fig.2. Fragment charge distributions measured for *p*(8.1GeV) + Au collisions and calculated for different values of the system volume, V_t, at the stage of fragment formation

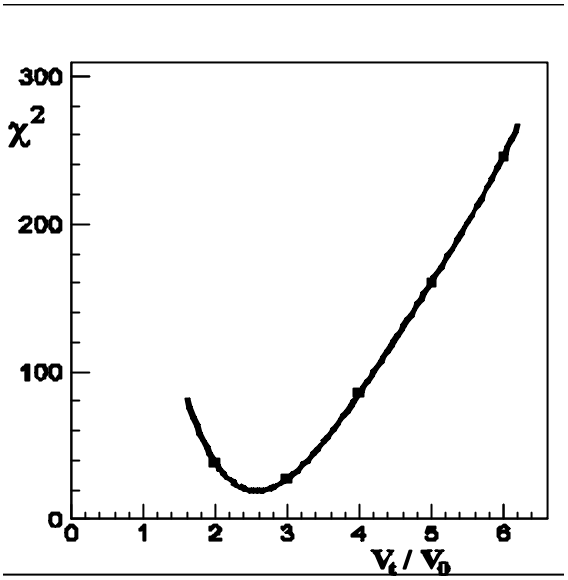

Fig.3. Value of χ^2 as a function of V_t/V_o for comparison of the measured and calculated IMF charge distributions. The best fit of the model prediction to the data corresponds to $V_t = (2.6 \pm 0.3)V_o$.

Figure 2 shows the IMF charge distribution for *p* (8.1GeV) + Au collisions measured by the telescope at $q \sim 87^o$, provided that at least one more IMF is detected by the setup. Error bars do not exceed the symbol size. The lines are obtained by calculations using the INC+Exp+SMM prescription under three assumptions about the fragmenting system volume: $2V_o$, $3V_o$ and $5V_o$. Only events with IMF multiplicity M=2 are considered. The theoretical charge distributions are normalized to get the total fragment yield equal to the measured one in the Z range between 3 and 11. A remarkable density dependence of the calculated charge

distributions is visible. The least-square method has been used for quantitative comparison of the data and the calculations. Figure 3 shows the normalized χ^2 as a function of V/V_o. From the minimum position and from the shape of the curve in its vicinity it is concluded that the best fit is obtained with the partition volume $V_t = (2.6 \pm 0.3)\ V_o$. The error bar (2s) is statistical in origin. This value corresponds to a mean density of the system $\rho_t = (0.38 \pm 0.04)\rho_o$ (see later why the subscript "t" is used).

3. SIZE OF EMITTING SOURCE

Generally, the fragment kinetic energy is determined by the thermal motion, Coulomb repulsion, rotation, and collective expansion, $E=E_{th} + E_C + E_{rot} + E_{flow}$. The Coulomb term is about three times larger than the thermal one [10]. The contributions of the rotational and flow energies are negligible for *p*+Au collisions [19]. So, the energy spectrum is essentially sensitive to the size of the emitting source. In the model, the fragment energy spectra are obtained by calculation of multi-body Coulomb trajectories, which starts with placing all charged particles of a given decay channel inside the freeze-out volume V_f. Each particle is assigned a thermal momentum corresponding to the channel temperature. The Coulomb trajectory calculations are performed for 3000 fm/*c*. After that the fragment kinetic energies are close to the asymptotic values [10]. These calculations are the final step of the INC+Exp+SMM combined model.

We analyzed carbon spectrum measured at $q \sim 87^o$ under the condition that at least one additional IMF is detected by FMD. Figure 4 gives a comparison of the measured spectrum with the calculated ones. The energy ranges of the spectra are restricted to 80 MeV to exclude the possible contribution of pre-equilibrium emission. The calculations are performed with a fixed break-up volume, $V_t = 2.6\ V_o$. The freeze-out volume, V_f, is taken as a free parameter.

Figure 4 shows the calculated spectra for V_f / V_o equals to 3, 6 and 13. The least-square method is used to find the value of V_f for the best description of the data. In Fig. 5, the value of χ^2 is given as a function of V_f / V_o. From the position of its minimum one gets $V_f = (5 \pm 1)$ V_o (mean freeze-out density $\rho_f \sim 0.2\ \rho_o$). Systematics provides the main contribution to the error of this estimation of the freeze-out volume. It is caused by a 5% uncertainty in the energy scale calibration. In our paper [16] the value $V_f = (11 \pm 3)$ V_o was obtained by analyzing the inclusive energy spectrum of carbon. This great difference may be explained by the fact that statistical model, SMM, overestimates fragment energies for events with M =1, as demonstrated in Ref. [20]. As result, the fitting procedure shifts V_f to the larger values.

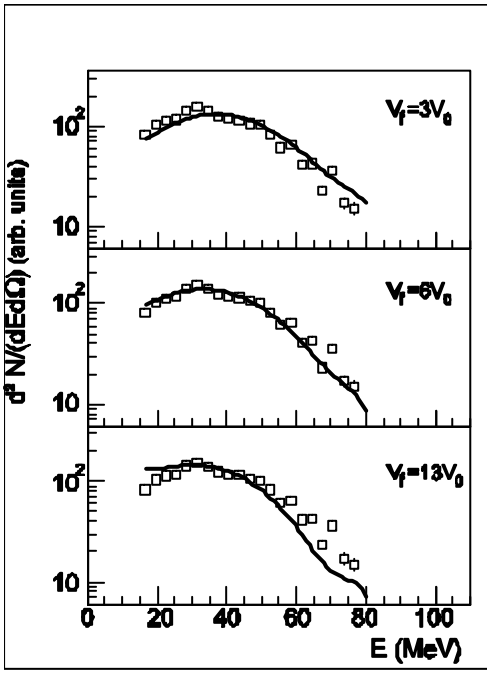

Fig.4. Kinetic energy spectrum of carbon emitted (at $q \sim 87^o$) by the target spectator in p(8.1GeV) + Au collisions. Symbols are the data, lines are calculated assuming freeze-out volume, V_f, to be equal to 3, 6, and 13 V_o.

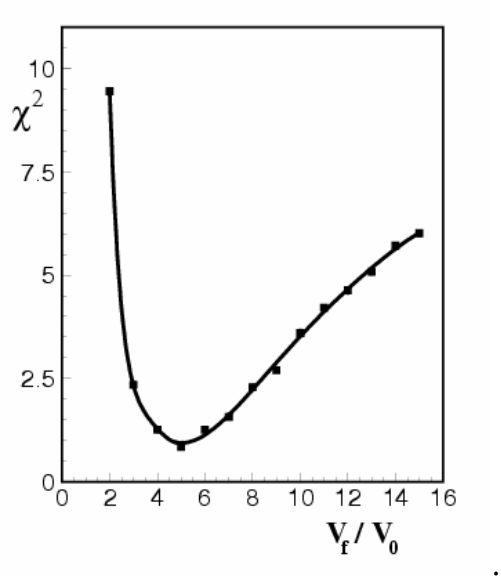

Fig.5. Value of χ^2 as a function of the freeze-out volume V_f / V_o for comparison of the measured and calculated kinetic energy spectra of carbon.

4. FRAGMENT EMISSION TIME

The time scale of IMF emission is a crucial characteristic for understanding the mechanism of this decay process: whether it is a "slow" successive and independent evaporation of IMF's or a multi-body decay mode with almost simultaneous ejection of the fragments governed by the total accessible phase space. "Almost simultaneous" means that all the fragments are liberated faster than the characteristic Coulomb time $\tau_c \approx 10^{-21}$s (400-500 fm/*c*) [21], which is the mean time of fragment acceleration in the Coulomb field of the system. In that case, emission of the fragments is not independent. They interact with each other via the Coulomb force during the acceleration in the common electric field. Thus, measurement of the IMF emission time τ_{em} (the mean time separation between two consecutive fragment emissions) is a direct way to answer the question as to the nature of the multifragmentation phenomenon.

There are two procedures to measuring the emission time: analysis of the IMF-IMF correlation function in respect to the relative velocity (see for example [24]) or in respect to the relative angle. We used the second method. Figure 6 shows the IMF-IMF relative angle

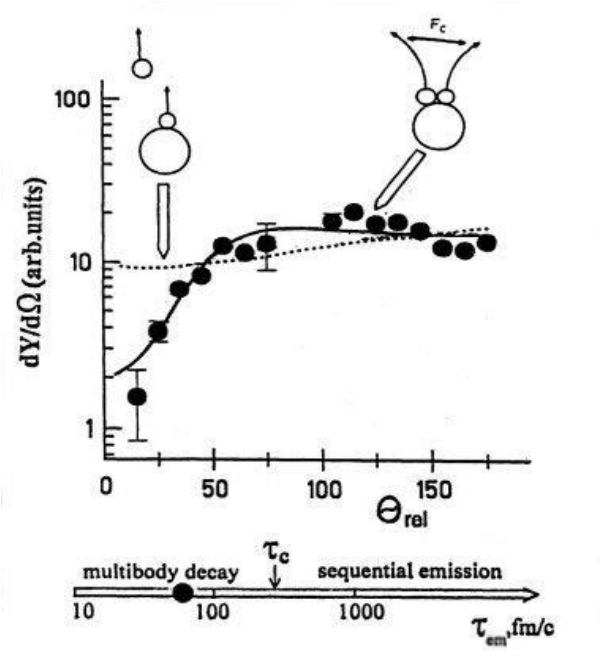

Fig.6. Distributions of relative angles between coincident IMF's for ^{4}He (14.6 GeV) + Au collisions. Solid line is calculated for the simultaneous emission of fragments, dashed line corresponds to the independent evaporation. Time axis is divided into two parts by the Coulomb time τ_c: multi-body decay is for $\tau_{em} < \tau_c$, and sequential evaporation is for $\tau_{em} > \tau_c$.

correlation for the fragmentation of target spectator in ^{4}He (14.6 GeV) + Au collisions [22,23]. The correlation function exhibits a minimum at $q_{rel}=0$ arising from the Coulomb repulsion between fragments from the same event. The magnitude of this effect drastically depends on the time scale of emission, since the longer the time distance between the fragments, the larger their space separation and the weaker the Coulomb repulsion. The multi-body Coulomb trajectory calculations fit the data on the assumption that the mean emission time is less than 75 fm/c ($2.3 \cdot 10^{-22}$ s). This value is significantly smaller than τ_c – the characteristic Coulomb time. Trivial mechanism of IMF emission (independent evaporation) seems to be definitely excluded.

More refined measurement of fragment emission time was done by FASA collaboration for p(8.1 GeV) + Au [10]: $\tau_{em}=(50 \pm 10)$ fm/c. Model dependence of result is carefully considered. Note that Ref. [22,23] are the first papers with experimental measurements of the characteristic time for the thermal multifragmentation. These were followed by a number of

similar studies [25,26]. The measured time scale of fragment emission is in accordance with the scenario of the spinodal decomposition.

5. FRAGMENTATION AND FISSION: SIMILARITIY AND DIFFERENCES

Figure1 presents the proposed spinodal region in the *T*-ρ *plane* [3] with the experimental data obtained by FASA collaboration. The points for the break-up and freeze-out configurations are located at ρ_t and ρ_f. Corresponding temperatures have been determined by fitting the data for fragment yields with the statistical model calculations [19]. The estimated value of the fragmentation barrier (~100 MeV) has been taken into account. The break-up point is deep inside the spinodal region, the top of which is specified by the critical temperature for the liquid-gas phase transition [11]. The point at ρ_f does not belong actually to the spinodal region, as it does correspond to a final channel configuration composed by fragments at normal density.

The existence of two different size characteristics for multifragmentation has a transparent meaning. The first volume, V_t, corresponds to the moment of fragment formation, when the properly extended hot target spectator transforms into a configuration consisting of specified pre-fragments. There are still links (nuclear interaction) between them. The final channel of disintegration is completed during the evolution of the system up to the moment when receding and interacting pre-fragments become completely separated. This is just as in ordinary fission. The saddle point (which has a rather compact shape) resembles the final channel of fission by way of having a fairly well-defined mass asymmetry. Nuclear interaction between fission pre-fragments ceases after descent of the system from the top of the barrier to the scission point. In papers by Lopez and Randrup [27] the similarity of both processes was used to develop a theory of multifragmentation based on suitable generalization

of the transition-state approximation first considered by Bohr and Wheeler for ordinary fission. The transition states are located at the top of the barrier or close to it. The phase space properties of the transition states are decisive for its further fate, for specifying the final channel.

Being conceptually similar to the approach of Ref. [27], the statistical model of multifragmentation (SMM) uses the size parameter, which can be determined by fitting to data. The size parameter obtained from the IMF charge distribution can hardly be called a freeze-out volume. In the spirit of the papers by Lopez and Randrup we suggest the term "transition state volume", V_t (see Fig. 7). The nuclear interaction between fragments is still significant when the system volume is equal to V_t, and only when the system has expanded up to V_f, are the fragments freezing out. In the statistical model used, the yield of a given final channel is proportional to the corresponding statistical weight. It means, that nuclear interaction between pre-fragments is neglected when the system volume is V_t, and this approach can be viewed as a rather simplified transition-state approximation. Nevertheless, the SMM describes well the IMF charge (mass) distributions for thermally driven multifragmentation.

The evidence for the existence of two characteristic volumes of multifragmentation changes the understanding of the time scale of the process. Now one can imagine the following ingredients of the total time scale: t_1 is the mean thermalizataion time of the excited target spectator, t_2 is the mean time of the expansion to reach the transition state, $(t_3 - t_2)$ is the mean time of descent of the system from the top of the barrier to the multi-scission point. The system configuration on the way to the scission point is composed from several pre-fragments connected by necks. Their random rupture is characterized by the mean time, t_n, which is an

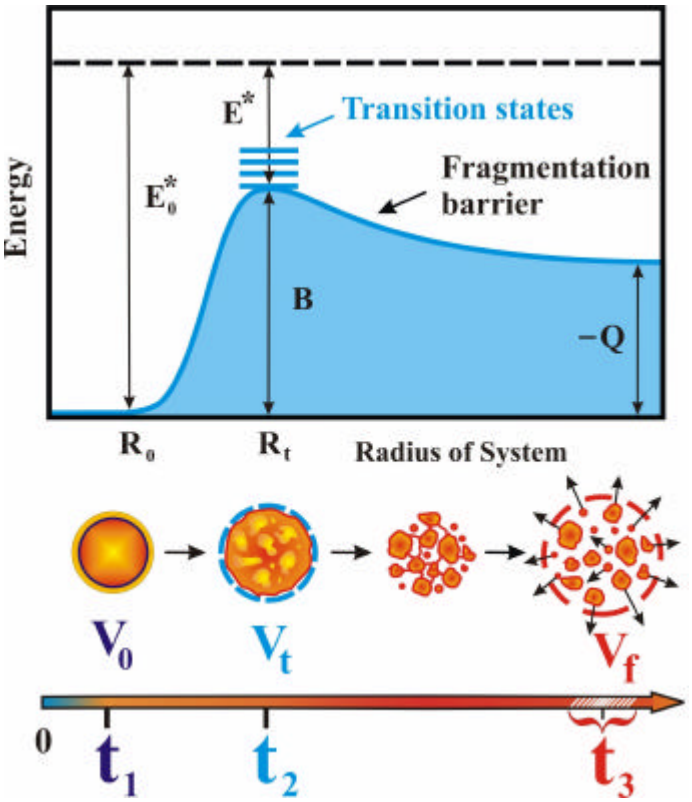

Fig.7. Upper: qualitative presentation of the potential energy of the hot nucleus (with excitation energy E_o*) as a function of the system radius. Ground state energy of the system corresponds to E=0, B is the fragmentation barrier, Q is the released energy. Bottom: schematic view of the multi-fragmentation process and its time scale.

important ingredient of the fragment emission time, τ_{em}. Another ingredient is characteristic time of the density fluctuations in the transition state, τ_d. So, $\tau_{em} \sim (\tau_d^2 + t_n^2)^{1/2}$. Formally t_{em} may be understood as the standard deviation of t_3: $\tau_{em} = (< t_3^2 > - < t_3 >^2)^{1/2}$. In the earlier papers, the emission time was related only to the time characteristic of density fluctuations in

the system at the stage of fragment formation, i.e. at $t \sim t_2$. The actual picture is much more complex.

What are the expected values of these characteristic times? Thermalization or energy relaxation time after intranuclear cascade, t_1, is model estimated to be (10 – 20) fm/*c* [28]. Expanding Emitting Source model (EES) predicts $\langle t_2 - t_1 \rangle \sim 70$ fm/*c* for *p* (8.1GeV)+Au collisions [29]. In this model, it is assumed, that $t_2 \sim t_3$. Fragment emission time, τ_{em}, is measured in many papers to be ~ 50 fm/*c*. The density fluctuation time, t_d, is model estimated to be 30-40 fm/c [30]. Calculation within the QMD model results in estimation of t_3 to be equal (150-200) fm/*c* [31]. A new theoretical consideration of the partition dynamic of very hot nuclei is needed. It is especially important to find a way to measure the value of t_3.

Note, that in the case of ordinary fission t_2 is specified by the fission width G_f, which corresponds to the mean time of order of 10^{-19}s (or ~ $3.3 \cdot 10^4$ fm/c) for the excitation energy around 100 MeV [32]. The value t_3 was model estimated in a number of papers (e.g. [33]): $t_3 \sim$ 1000 fm/c. A mean neck rupture time is estimated in [34] within the model of Rayleigh instability: $\tau_n = [1.5(R_n/\text{fm})^3]^{1/2} \cdot 10^{-22}$ s . The values of τ_n for fission are found to be less than 300 fm/c. Using eq.(1) for the estimation of the mean time for the multi-neck rupture in the multifragmentation, one gets t_n between 40 and 115 fm/c under assumption of the neck radius R_n between 1 and 2 fm. These estimations are in qualitative agreement with the measured values of the fragment emission time τ_{em}.

The relative elongation of the very heavy systems (Z>99) at the fission scission point is similar to that for the multi-scission point of medium hot nuclei (rare earth region). For the fission of the lighter nuclei, (Po–Ac), the scission elongation is larger [34].

6. SUMMARY

Spinodal decomposition of hot nuclei is interpreted as a *liquid-fog* phase transition with the final state consisting of droplets (IMFs) with nuclear gas interspersed between them.

Analysis of the exclusive data for the fragmentation in *p*(8.1GeV) + Au collisions results in the conclusion that there are *two* characteristic volume parameters of the process. One, $V_t = (2.6 \pm 0.3)\ V_o$, is obtained from the IMF charge distribution. It corresponds to the configuration of the system at the stage of pre-fragment formation. It is similar to the saddle point in ordinary fission. Volume V_t can be called as a "chemical freeze-out volume". The other, $V_f = (5 \pm 1)\ V_o$, is found from the analysis of the fragment energy spectra. It is the kinetic freeze-out volume corresponding to the multi-scission point in terms of ordinary fission. The obtained values are model dependent. There are some papers (e.g. [35,36]), which are based on the suggestion that fragments are produced at an early, high temperature and high density stage, in contrast to the statistical model SMM used in the present study. So, there is a room for further investigation of this issue.

The authors are grateful to A. Hrynkiewicz, A.I. Malakhov, A.G. Olchevsky for support. The research was supported in part by the Russian Foundation for Basic Research, Grant ? 03-02-17263 and the Grant of the Polish Plenipotentiary to JINR.

REFERENCES

[1] J.P. Bondorf, A.S. Botvina, I.N. Mishustin et al., Phys. Rep. 257, 133 (1995).
[2] D.H.E. Gross, Rep. Progr. Phys. 53, 605 (1990).
[3] G. Sauer, H. Chandra and U. Mosel, Nucl. Phys. A264, 221 (1976).
[4] H. Jaqaman, A.Z. Mekjian and L. Zamick, Phys. Rev. C 27, 2782 (1983).
[5] P.J. Siemens, Nature 305 (1983) 410; Nucl. Phys. A 428, 189c (1984).
[6] K.A. Bugaev et al., Phys. Rev. C 62, 044320 (2000).
[7] V.E. Viola, Nucl. Phys. A 734, 487 (2004).
[8] B. Borderie et al., Nucl. Phys. A 734, 495 (2004).
[9] J.D. Frankland et al., Phys.Rev. C 71, 034607 (2005).
[10] V.K. Rodionov et al., Nucl. Phys. A 700, 457 (2002).

[11] V.A. Karnaukhov et al., Nucl. Phys. A 734, 520 (2004).
[12] Bao-An Li, D.H.E. Gross, V. Lips and H. Oeschler, Phys. Lett. B 335, 1 (1994).
[13] J.B. Natowitz et al., Phys. Rev. C 66, 031601(R) (2002).
[14] M.D. Agostino et al., Nucl. Phys. A 699, 795 (2002).
[15] A. Raduta et al., arXiv: nucl-th/0503005 v1 (2005)
[16] V.A. Karnaukhov et al., Phys. Rev. C 70, 041601(R) (2004).
[17] V.A. Karnaukhov et al., Nucl. Phys. A 749, 65c (2005).
[18] V.D. Toneev et al., Nucl. Phys. A519, 463 (1990).
[19] S.P Avdeyev et al., Nucl.Phys. A709, 392 (2002).
[20] H. Oeschler et al, Part. and Nucl., Lett. ? 2[99], 70 (2000).
[21] O. Shapiro and D.H.E. Gross, Nucl.Phys.A 573, 143 (1994).
[22] S.Yu. Shmakov et al. Phys. At. Nucl. 58,1635 (1995).
[23] V.Lips et al., Phys. Lett. B. 338, 141 (1994).
[24] D.R. Bowman et al., Phys. Rev. C 52, 818 (1995).
[25] G. Wang et al.,Phys. Rev. C 57, R2786 (1998).
[26] L. Beaulieu et al., Phys.Rev.Lett. 84, 5971 (2000).
[27] J.A. Lopez and J. Randrup, Nucl. Phys. A503, 183 (1989);
Nucl. Phys. A512, 345 (1990).
[28] B. Borderie, Preprint Orsay/IPNO-DRE-92-03 (1992).
[29] S.P. Avdeyev et al., Eur. J. Phys. A 3, 75 (1998).
[30] G. Wang et al., Phys.Rev. C 53, 1811 (1996).
[31] V. Baran et al., Nucl. Phys. A 703, 603 (2002).
[32] F. Goldenbaum et al., Phys.Rev. C 82, 5012 (1999).
[33] D. Hilscher, H. Rossner, Annales de Phys. 17, 471 (1992).
[34] U. Brosa et al., Phys. Rep. 197, 162 (1990).
[35] C. Dorso and J.Randrup , Phys. Lett. B 301, 328 (1993).
[36] X. Campi et al., Phys.Rev. C 67, 044610 (2003).